Catalysis Letters (2024) 154:1050–1060
https://doi.org/10.1007/s10562-023-04333-y

N-doped Metallocene Catalysts for Synthesis of High Quality Lubricant Base Oils from Fishcher–Tropsch Synthesized α-Olefin

Bingyu Shi[1,2] · Man Liu[1] · Jiangang Chen[1]

Received: 12 December 2022 / Accepted: 24 March 2023 / Published online: 30 May 2023

Abstract

Derivatives of 2,4-dimethyldihydrocyclopentadiene were prepared, characterized by NMR spectroscopy, which was applied to 1-decene oligomerization. A two-step activation method in which both triisobutylaluminium (TIBA) and methyl aluminoxane (MAO) were co-used in sequence particularly been developed for N-doped ligand catalyst. N-doped catalyst had a very high polymerization conversion at 60–110 °C by varying the reaction temperature at 20 eq. of TIBA and 100 eq. of MAO, reaching 89.95% at 80 °C. In addition, oligomers with different viscosity grades could be obtained by adjusting the temperature. At optimized reaction conditions 75 °C, 10 eq. of TIBA and 50 eq. of MAO activation, the single pass conversion of 91.33% was achieved. The obtained oligomers had a high viscosity index above 170 at $KV^{100} = 6$. In addition, the two-step activation method was used to compare with the conventional one-step activation method on catalysts with three different ligands of zirconium chloride. A high catalytic productivity was achieved by the two-step activation process. Depending on the nature of the ligands used, β-hydride elimination, 2,1 insertion and 1,2 rearrangement were detected as main chain release mechanisms. Meanwhile, the pathways of oligomer formation were also summarized. In brief, N-doped complex is promising catalysts for the production of high quality lubricant base oils due to their high catalytic activity and high thermal stability.

Graphical Abstract

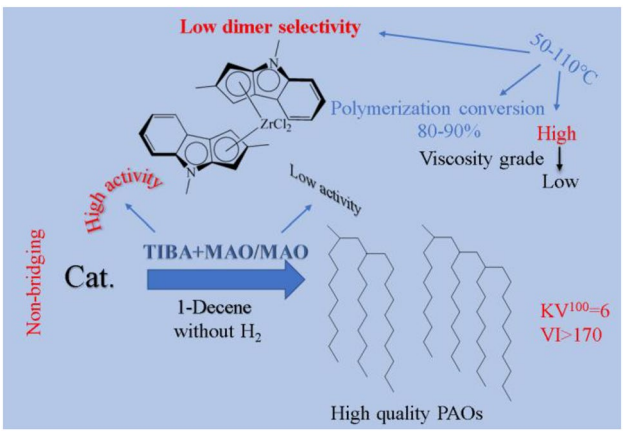

Keywords Metallocene catalysts · Chain release mechanisms · 1-decene · N-doped · PAO

1 Introduction

In recent years, as heavy loading transportation, extreme speed machinery and fine equipment continue to upgrade, which in turn challenges the performance of lubricants. Traditional mineral base stocks no longer meet the requirements of today's equipment. Compared to conventional mineral base oils [1], poly-alpha-olefins (PAO) [2] have excellent viscosity–temperature characteristics and low-temperature fluidity owing to their unique long straight chain alkane backbone and multiples side chain structure when

Extended author information available on the last page of the article

used as lubricant base oils [3, 4]. Meanwhile, the special molecular structure prevents the hydrocarbons from being oxidized by the quaternary carbon atoms in the surrounding media [5], which enables PAO to have excellent biodegradability and ultimately makes it an excellent environmental material [6, 7]. In addition, Coal-based Fischer–Tropsch technology (FTS) [8], in coal-rich and oil-poor countries such as China, is being considered as an important way to produce value-added chemicals to ease the pressure of energy imports. Long-chain α-olefins, an important product of the FTS [9], have been explored extensively by researchers in recent years, and excellent product yields have been obtained. Hence, the development of excellent catalysts for the polymerization of FTS long-chain α-olefins to form PAO provided the possibility for the efficient exploitation of coal resources.

The level of viscosity index (VI) is used to evaluate the sensitivity of a lubricant base oil to changes in ambient temperature. Consequently, one of the research objectives of researchers is to obtain lubricant base oils with as high a viscosity index as possible through process optimization for use in more severe environmental changes. This index is determined by the standard method ASTM D-2270 and is calculated by measuring the kinematic viscosity values of the oil at 40 °C (KV^{40}) and 100 °C (KV^{100}). Compared to conventional mineral base oils (VI values ~ 90), the higher VI values of poly-alpha-olefin lubricant base oils are significantly higher, around 160 [2, 10]. Thereby, to relieve the dependence of lubricant performance on ambient temperature, the development of synthetic PAO synthesis processes with high VI values has wide application prospects. Currently, metallocene catalysts [11], Ziegler–Natta catalysts [12], and so on, have been developed and successfully used in α-olefin polymerization reactions. Among them, metallocene catalysts are designated as powerful catalysts for α-olefin polymerization because of their ultra-high activity, single active center [13], and products with excellent viscosity–temperature characteristics and oxidative stability.

However, conventional metallocene catalyst ($LZrCl_2$) catalysis requires a large amount of co-catalyst (MAO 100–10,000 equivalents) to achieve the desired activation effect [14, 15], resulting in high costs in lubricant base oil synthesis. In addition, the dimer content of $LZrCl_2$ catalyst synthesis products is predominant [16] and leads to low VI values of lube base oils. Most conventional metallocene catalysts are synthesized using cyclopentadiene as a ligand. Interestingly, a cyclopenta[b]thiophene catalyst was successfully applied to α-olefin polymerization reactions [5, 17, 18]. In the S-doped metallocene catalytic system, a two-step activation method was developed, which greatly reduced the amount of co-catalyst (MAO) and improved the economics of the catalytic reaction. However, the research of heteroatom-modified metallocene in

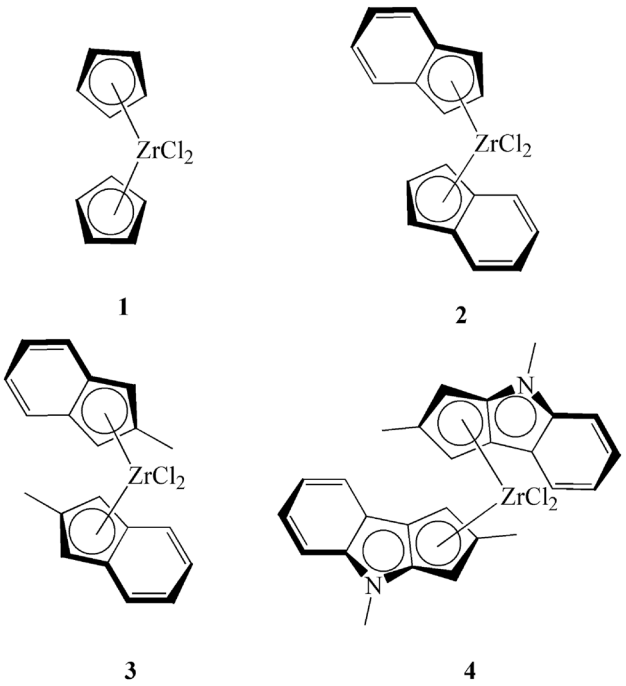

Scheme 1 Zirconocenes studied in the oligomerization of 1-decene

α-olefin polymerization reactions is still in its infancy and there is much concern for the selective obtaining of trimer-tetramer fractions to obtain high quality PAO [19]. Therefore, the development of more environmentally friendly and cheaper heteroatomic metallocene catalysts is of great importance for the polymerization of long-chain α-olefins into high quality lubricant base oils.

In this work, we developed a novel nitrogen-doped metallocene catalyst for the polymerization of long-chain α-olefins to synthesize high-performance lubricant base oils. The modulation factors of the reaction performance and the polymerization mechanism of N-doped catalysts were systematically investigated using gas chromatography (GC), Fourier Transform Infrared Spectrometer (FTIR), ^{1}H NMR, ^{1}C NMR and Gel Permeation Chromatography (GPC)techniques. Meanwhile, the chain release mechanism involved in the catalytic polymerization pathway was investigated. The catalytic results showed that the synthesized N-doped catalyst obtained 91.33% conversion under mild reaction conditions (T = 75 °C, eq. TIBA = 10, eq. MAO = 50) compared with the performance of conventional metallocene catalysts. This work points to a new direction for the development and exploitation of novel catalysts for the polymerization of long-chain α-olefins (Scheme 1).

2 Experimental Section

2.1 Solvents, Reagents and Catalysts

Ether refluxed on Na/benzophenone, CH_2Cl_2 refluxed on CaH_2, *n*-hexane stored in Na, all distilled under argon before use. 1-decene was dried with CaH_2 at 100 °C with stirring for 24 h and then distilled under argon under reduced pressure. MAO (1.0 M toluene solution) and TIBA (1 M hexane solution) were purchased from Shandong Yanfeng New Material Technology Co. *n*-Butyllithium (1.6 M hexane solution), zirconium tetrachloride, 1-methylindole, methanesulfonic acid, phosphorous pentoxide, lithium aluminum hydride and p-toluenesulfonic acid (TsOH) were purchased from Shanghai Aladdin Biochemical Technology Co. Complex **1** was procured from Shanghai Aladdin Biochemical Technology Co. All synthetic experiments were carried out in an argon atmosphere using a glove box and Schlenk technique. All solvents were subjected to dehydration and de-oxygenation prior to use. Complexes **2** [20, 21] and **3** [22] were synthesized according to previous reports.

2.2 Analysis

$CDCl_3$ was purchased from (Shanghai Aladdin Biochemical Technology Co., Ltd., D99.8%). ^{1}H NMR spectra of ligands, catalysts, and polymers were recorded on a Bruker AVANCE III 400 spectrometer (400 MHz) at 20 °C. Chemical shifts are reported in ppm relative to solvent residual peaks. The number average molar mass (M_n) and mass average molar mass (M_w) of the oligomers were determined using an Agilent GPC 1260 Infinity gel permeation chromatograph equipped with a MIXED-E column and a 100A column. THF was used as the eluent (1 mL/min). A universal calibration was performed at 40 °C according to the polystyrene standard and the measurements were recorded.

The product distribution of the 1-decene oligomers produced in the catalytic reaction with zirconium dichloride was determined by gas chromatography. The polymerization conversion of olefins is obtained by material equilibrium and is influenced by some incidental side reactions. One of them is the isomerization of the initial α-olefin; the other is the formation of *n*-alkanes. Therefore, we have calculated the olefin conversion, the content of by-products and the relative content of target oligomer fractions (P_n3–5) and summarized them in the Supporting Information Tables S1–S3. The analysis was carried out by gas chromatography with a hydrogen flame ionization detector Shimadzu GC-2010.

The kinematic viscosity (KV) of the polymers at 40 °C and 100 °C was measured by passing a volume of liquid through a calibrated capillary flow meter under gravity using an RP-265G-2 viscometer. The viscosity index (VI) values were calculated according to the ASTM D-2270 method. FTIR was tested by a Bruker TENSORII spectrometer from Germany with a resolution of 4 cm^{-1}. The Fourier infrared spectroscopy (FTIR) spectral range was 4500–500 cm^{-1}.

2.3 Complex 4 Preparation

All the synthetic reactions were carried out under argon atmosphere. 2,4-dimethyldihydrocyclopenta[b]indole ligands were synthesized as previously reported [23, 24] and the specific synthesis procedure is shown below.

2.3.1 2,4-Dimethyl-1,2,3,4-Tetrahydrocyclopenta[b] indol-3-one

Stir 24.3 mL (36 g) of methanesulfonic acid with 3.6 g of phosphorus pentoxide at 50 °C for 2 h until thoroughly dissolved. A mixture of 15 mL (0.12 mol) of 1-methylindole, 10.18 mL (0.12 mol) of methacrylic acid and 15 mL of dichloromethane was slowly added dropwise at 95 °C and reacted at 75 °C for 3 h. After cooling and quenching with distilled water, the crude product was extracted with ether to separate the organic and aqueous phases. The organic phase was washed with $NaHCO_3$ solution and dried over anhydrous Na_2SO_4 and concentrated. Purification on a silica gel column (*n*-hexane/ethyl acetate (8/1) mixture as eluent) gave 12.57 g of dark yellow oil. Yield: 52.64%. ^{1}H NMR (δ, $CDCl_3$, 25 °C):7.7 (d, J = 8.0 Hz, 1H, CH) 7.5–7.1 (m, 3H,), 3.9 (s, 3H, $-CH_3$), 3.3 (dd, J_1 = 8.0 Hz, J_2 = 16.0 Hz, 1H, $-CH_2-$), 3.0 (m, 1H, CH), 2.65 (dd, J_1 = 2.0 Hz, J_2 = 17.0 Hz, 1H, $-CH_2-$) 1.37 (d, J = 8.0 Hz, 3H, $-CH_3$). Anal. Found: C, 78.85; H, 7.25; N, 6.91. Calcd ($C_{13}H_{13}NO$): C, 78.36; H, 6.58; N, 7.03 (the ^{1}H NMR spectra are provided in Supporting Information, Fig. S1).

2.3.2 2,4-Dimethyldihydrocyclopenta[b]indole

Lithium aluminium hydride (1.14 g, 0.03 mol) was suspended in 100 mL of ether under an argon atmosphere in an ice bath. 2,4-Dimethyl-1,2,3,4-tetrahydrocyclopenta[b] indol-3-one (6 g, 0.03 mol) dissolved in 30 mL of ether was added slowly and reacted at room temperature for 2.5 h. It was decomposed with ammonium chloride solution. The aluminium hydroxide was filtered off and the organic phase was separated, washed with distilled water and dried with anhydrous Na_2SO_4. After concentration, the resulting alcohol can be used without further purification. The corresponding alcohol (5 g) was dissolved in benzene (100 mL), TsOH (0.017 g) was added and refluxed with a Dean–Stark apparatus until no water bubbles sank. The reaction mixture

was cooled and the organic layer was washed with $NaHCO_3$ and dried over anhydrous Na_2SO_4 and concentrated. The crude product was purified by chromatography using a silica gel column (hexane/ethyl acetate (10/1) mixture as eluent). The yellow oil was 2.03 g. Yield 44.37%. ^{1}H NMR (δ, $CDCl_3$, 25 °C): 7.45 (d, J = 9.0 Hz, 1H, CH), 6.95–7.25 (m, 3H, CH), 6.35 (s, 1H, CH), 3.68 (s, 3H, N–CH_3), 3.13 (s, 2H, –CH_2–), 2.15 (m, 3H, –CH_3). ^{13}C NMR ($CDCl_3$, 20 °C) δ: 148.83; 148.45; 139.1; 123.32; 118.18; 117.87; 116.33; 115.64; 115.06; 108.57; 35.57; 29.74; 16.62. Anal. Found: C, 85.30; H, 7.33; N, 7.37. Calcd ($C_{13}H_{13}N$): C, 85.21; H, 7.15; N, 7.64 (the ^{1}H and ^{13}C NMR spectra are provided in Supporting Information, Figs. S2 and S3, respectively).

2.3.3 Bis(2,4-dimethylcyclopentadienyl[b]indolyl) zirconium dichloride

First, 1 g (5.46 mmol) of 2,4-dimethyl-1,4-dihydrocyclopentadieno[b]indole ligand was dissolved in 20 mL of ether and stirred for 5 min. The solution was cooled to − 78 °C and then 3.76 mL (1.6 M hexane solution, 6 mmol) of *n*-butanol was added slowly dropwise and stirred for 12 h at room temperature. The solution was then cooled to − 40 °C. $ZrCl_4$ (0.636 g, 2.73 mmol) was added and the mixture was stirred at room temperature for 5 h and filtered. The volatiles were removed under reduced pressure and the residue was dissolved in 20 mL of CH_2Cl_2 and hexane was added dropwise at room temperature until it started to crystallize. The resulting mixture was stored at − 20 °C for 2 days and the residue was removed under reduced pressure to give 0.62 g of a solid yellow–brown powder product in 43.26% yield. Isomer I: ^{1}H NMR (δ, $CDCl_3$, 25 °C): 7.94 (d, J = 8.0 Hz, 1H, CH), 7.42–7.08 (m, 3H, CH), 6.18 (s, 1H, CH), 5.69 (s, 1H, CH), 3.8 (s, 3H, N–CH_3),1.35 (s, 3H, –CH_3). Isomer II: ^{1}H NMR (δ, CDCl3, 25 °C): 7.32–6.99 (m, 3H, CH),6.93 (d, J = 8.0 Hz, 1H, CH), 6.05 (s, 1H, CH), 5.8 (s, 1H, CH), 3.56 (s, 3H, N–CH_3), 2.32 (s, 3H, –CH_3). ^{13}C NMR ($CDCl_3$, 20 °C) δ: 147.11; 145.87; 145.34; 144.41; 131.95; 130.13; 125.11; 125.05; 120.33; 120.04; 119.37; 119.12; 110.8; 109.75; 109.29; 109.05; 96.47; 96.13; 94.35; 92.11; 31.6; 31.2; 17.61; 16.11 (the ^{1}H and ^{13}C NMR spectra are provided in Supporting Information, Figs. S4 and S5, respectively).

2.4 Oligomer Preparation and Characteristics

All polymerization reactions were carried out under argon atmosphere. For the activation using the one-step method, bisindene zirconium dichloride was used as the main catalyst and 1-decene as the feedstock. 2 mL of toluene was added to the feedstock to dissolve the complex, heated to the specified temperature and stirred for 10 min. Then add 90 eq. of MAO. stir at the specified temperature, stop heating after a certain time, cool for 5 min and terminate the reaction by adding 5% hydrochloric acid/ethanol solution. The organic phase was separated by extraction and dried, and the solvent and unreacted monomers were removed by vacuum distillation. When using the two-step activation method, the complex 4 was used as the main catalyst and 1-decene were used as raw materials. 20 eq. of TIBA was added to the feedstock, heated to the specified reaction temperature and stirred for 20 min. Then 50 eq. of MAO was added, stirred at the specified temperature, and the heating was stopped after a certain time, and the reaction was terminated by adding 5% hydrochloric acid/ethanol solution after cooling for 5 min. The organic phase was separated by extraction and dried, and the solvent and unreacted monomers were removed by vacuum distillation.

3 Results and Discussions

3.1 Analysis of the Mechanism of End Group Formation and Chain Release

The chain release mechanism is an important issue in monocentric α-olefin coordination and insertion polymerization catalysis, as it involves controlling the molecular weight and the structure of the chain-end groups of the olefin polymerization product. The conventional chain release mechanism is discussed as shown in Scheme 2. In the presence of aluminum co-catalysts, various chain transfer reactions may produce saturated end groups and different unsaturated end groups. In general, the formation of saturated end groups by chain transfer to aluminum is one of the common chain termination reactions under conditions where hydrogen is not involved in the reaction as a chain transfer reagent (Scheme 2, 1). This chain release mechanism is mainly discussed in the literature [25]. And chain transfer to aluminum is the only chain release mechanism for the [μ-dimethylsilylbis(η^5-2,5-dimethyl-7H-cyclopentadienyl) [1,2-b:4, 3-b′]dithiophen-7-yl)]zirconium dichloride/TIBA/MAO catalyzed system at 60 °C [26]. For the formation of unsaturated chain end groups, this can occur through different pathways. Bergman [27, 28] earlier proposed the transfer of β-hydride to Zr to form zirconium–hydrogen complexes by reacting with two olefin molecules, resulting in selective dimerization of α-olefins (Scheme 2, 2). For the polymerization of long-chain α-olefins. It can be terminated by β-hydride elimination or chain transfer to the monomer to form vinylidene chain ends (Scheme 2, 3) and also by β-alkyl elimination to form vinyl chain ends (Scheme 2, 4) [29]. Janiak [30] proposed that β-alkyl elimination is related to the spatial site resistance of the catalyst. And there are two channels for the formation of double bonds at the internal terminal groups. One is the formation of trisubstituted

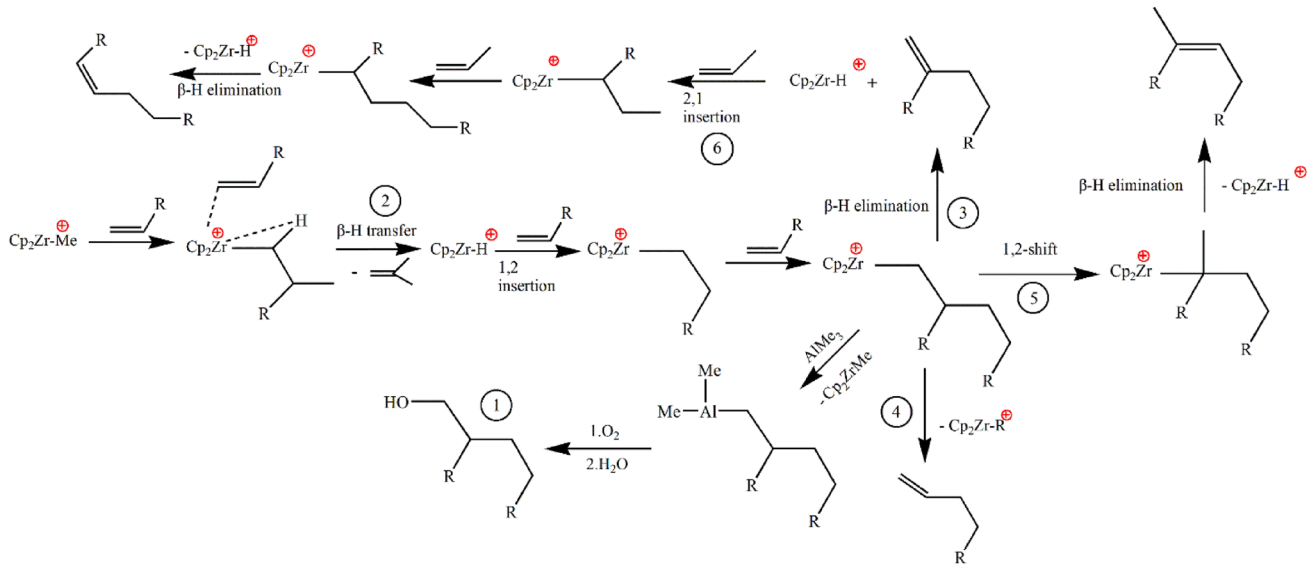

Scheme 2 Traditional chain release mechanism in α-olefin polymerization

double bonds through 1,2-rearrangement (Scheme 2, 5) [31]. The second one is interpreted through cycloalkyl complexes, which are products formed by the monomeric insertion of Cp_2ZrH via 2,1-followed by the termination of chain-end reactions by β-hydride elimination (Scheme 2, 6) [5].

The polymerization products synthesized in this study were also analyzed by ^1H NMR to obtain the end groups and internal double bonds (Fig. S5, Supporting Information) represents the hydrogen spectrum of poly(1-decene). It can be seen from the figure that poly(1-decene) has three different types of proton peak signals: $–CH_3$ located between 0.8 and 1.0 ppm, $–CH_2–$ located between 1.0 and 1.7 ppm and protons bound to tertiary carbon (CH) located between 1.8 and 2.1 ppm. Information on the unsaturated chain ends can be detected in the high chemical shift region. The characteristic signals are 4.60–4.80 ppm for vinylidene fragments $>C=CH_2$, 4.9–5.05 ppm for vinyl fragments $–C=CH_2$, 5.05–5.20 ppm for trisubstituted fragments >C=CH–, and 5.3–5.45 ppm for internal-CH=CH– fragments [32, 33]. The end-groups appearing in the ^1H NMR results of the products were likewise supported by FTIR spectra (Fig. S8, Supporting Information).

3.2 Comparison of 1-Decene Oligomerization by Different Catalysts

When soluble $LZrCl_2$ is used as a catalyst in α-olefin polymerization experiments, a large amount of MAO is usually required for activation. The conventional one-step method activated only by using MAO was found to be unable to convert the insoluble $LZrCl_2$ into the active soluble form. Therefore, we used a two-step activation method in our experiments. For the conventional metallocene $LZrCl_2$ complexes (1, 2, and 3), two activation methods were experimentally investigated using two activation methods. In the two-step method, all $LZrCl_2$ complexes formed a homogeneous phase in 1-decene feedstock with 80 °C, 20 eq. of TIBA. However, the polymerization reaction was not detected. After the addition of a certain equivalent amount of MAO, all catalytic systems started to undergo polymerization reactions. To investigate the effect of these two activation methods on the catalytic activity and product distribution. The catalytic performance of four catalysts pretreated by both activation methods was investigated under the given conditions, and the results are summarized in Table 1.

Under the given reaction conditions, complexes 1–4 showed different polymerization behavior. Among them, when using the conventional activation method, complexes 1,2,3 showed no detectable polymerization products in the system when only 10 equivalents of MAO were used. The conversion of the catalysts remained low when the amount of MAO was continuously increased up to 50 equivalents, with 1.82%, 17.54%, and 9.52%, respectively. Compared to the conventional activation method, there was a significant increase in the conversion of complexes 1,2,3 with 40.49%, 46.9%, and 37.45%, respectively, when using the two-step activation method. Surprisingly, the N-doped complex 4 had a high conversion of 79.22% at low Al_{MAO}/Zr (Table 1, run 20). Meanwhile, the highest conversion of 90.4% was obtained when the value of Al_{MAO}/Zr was consistently increased to 50 equivalents (Table 1, run 21).

Complex 1 mainly catalyzed the formation of the 1-decene dimer. The selectivity reached 96.84% at 10 equivalents of MAO, activated by 20 equivalents of TIBA

Table 1 Oligomerization of 1-decene catalyzed by 1,2,3 and 4 (reaction time 4 h, 80 °C, 1-decene/Zr = 3×10^4)

Run	Cat	Al_{MAO}/Zr	Al_{TIBA}/Zr	Conv., %[a]	% Selectivity of oligomers in the reaction mixture after 4 h, for P_n				M_n[c]	M_w[c]	KV^{40}, cSt	KV^{100}, cSt	VI
					2[b]	3[b]	4[b]	5[b]					
1	**1**	10	–	–	–	–	–	–	–	–	–	–	–
2		50	–	1.8	87.8	6.1	3.9	2.3	–	–	–	–	–
3		90	–	43.9	90.8	7.2	1.7	0.3	373	453	5.25	1.90	–
4		10	20	40.5	96.8	1.9	0.8	0.5	345	378	4.83	1.72	–
5		50	20	56.5	88.7	8.3	2.1	0.9	377	456	5.46	1.94	–
6		90	20	62.5	76.8	15.2	5.5	2.5	384	480	6.08	2.02	133
7	**2**	10	–	–	–	–	–	–	–	–	–	–	–
8		50	–	17.5	39.6	25.3	19.6	15.5	895	2257	–	–	–
9		90	–	53.4	44.2	25.4	18.4	12.0	891	2135	34.44	6.74	158
10		10	20	46.9	42.0	26.6	18.8	12.6	767	1695	21.33	4.95	167
11		50	20	80.4	40.4	29.1	18.5	12.0	1028	2396	46.28	8.94	177
12		90	20	81.4	35.8	30.0	20.4	13.9	1271	3248	92.38	15.48	179
13	**3**	10	–	–	–	–	–	–	–	–	–	–	–
14		50	–	9.5	59.0	26.4	10.7	4.0	899	2327	–	–	–
15		90	–	66.1	68.4	20.4	7.9	3.4	647	1216	15.89	4.11	171
16		10	20	37.5	44.9	30.5	16.6	8.0	812	2144	29.53	6.62	191
17		50	20	75.2	45.2	28.1	15.6	11.2	777	2473	34.09	7.26	185
18		90	20	85.6	39.3	30.9	17.6	12.3	1065	2493	35.02	7.45	187
19	**4**	90	–	–	–	–	–	–	–	–	–	–	–
20		10	20	79.2	26.0	30.3	25.1	18.6	1267	2294	63.21	11.94	188
21		50	20	90.4	24.5	30.2	24.2	20.6	1341	3412	86.25	15.45	191
22		90	20	89.3	19.6	30.5	25.6	24.3	1460	3622	106.42	17.42	181

[a]Polymerization conversion of olefins

[b]GC data

[c]By GPC (THF)

(Table 1, Run 4). This is in agreement with the work of Nifant'ev et al. [34]. The dimer selectivity of complexes 2, and 3 under the same conditions was 41.98%, and 44.93%, respectively. Significantly, the N-doped complex 4 had a significantly lower dimer content of 26.03% compared to catalysts. This may be attributed to the fact that the introduction of N increases the electrophilicity of the Zr^+ cation active center of the catalyst, making the transfer rate of olefins smaller than the insertion rate of olefins. The higher dimer selectivity of complex 3 than complex 2 may be explained by the fact that the addition of methyl increases the spatial site resistance and decreases the electrophilicity of the active center of the catalyst, thus, inhibiting the insertion of olefins and decreasing the rate of chain growth. In agreement with previous reports[35], experiments using conventional activation methods for complexes 1–3 all exhibited that increasing the ratio of Al_{MAO}/Zr resulted in the formation of a large number of oligomers in the products (e.g. Table 1, Run 15). In contrast, all catalysts treated with the two-step activation method showed a decrease in dimer selectivity in the product as the Al/Zr ratio increased, and the measured M_w was consistent with this phenomenon. Nifant'ev et al. [36, 37] suggested that the increase in Al/Zr causes a gradual change to the active species from zirconium–aluminum chloride hydride complex A to dihydride complex B. In general, the presence of μ-Cl in species A allows the Zr active center in A to be less electrophilic and more closed than the Zr active center in B, which leads to a smaller rate of olefin insertion into A than the rate of B (Scheme 3). As a result, the dimer content is selectively reduced at high Al/Zr ratios. Meanwhile, the team developed a DFT theoretical model of this mechanism, which treats catalytic particles as cationic species with liganded R_2AlX fragments (X = H, F, Cl, Me). In the absence of R_2AlX ligand, oligomerization reaction is the better reaction pathway. When X = H, the highly stable β-agostic complex I-2X_bo is produced and the dimer is formed slowly. When X = Cl, it is the main pathway for dimer formation. And the β-hydride elimination of the transition state of TS-4X (X = H, Cl) shows a significant Zr–Al synergistic effect [38, 39]. The results of the kinematic viscosity tests of the polymerized products showed that the products obtained for complex 1 almost always had

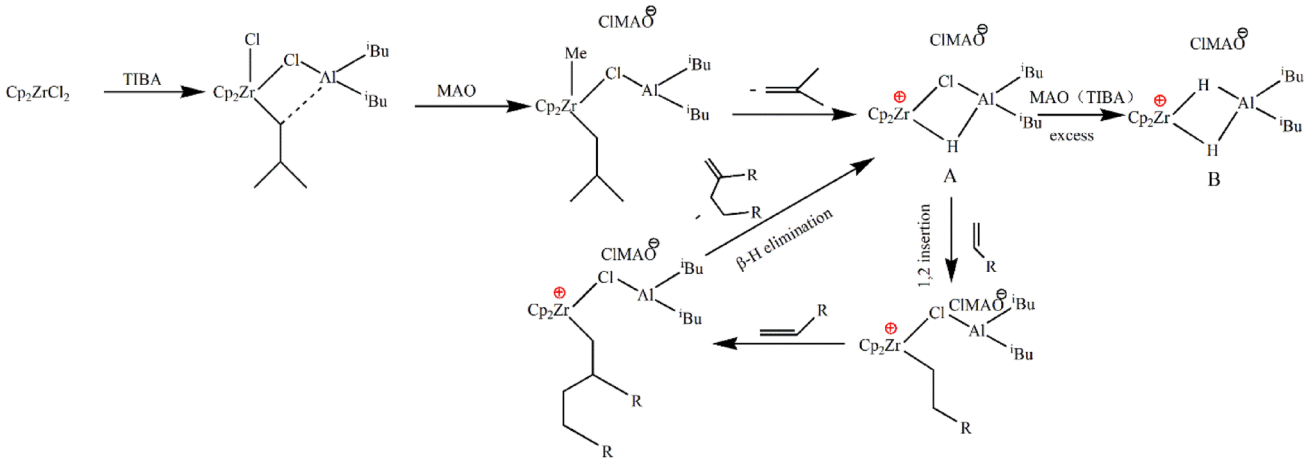

Scheme 3 Reaction mechanism of 1-decene polymerization catalyzed by zirconium chloride/TIBA/MAO catalytic system

a kinematic viscosity of fewer than 2 mm^2/s at 100 °C and were not suitable as lubricant base oils. For complexes 2 and 3, the VI values of the polymerized products were lower. However, the VI of the polymerized products increased significantly after the two-step activation treatment.

The results of ^1H NMR end-group analysis of poly-1-decene are provided in Fig. 1. For complex 1, four release mechanisms were detected. They are β-hydride elimination (2), β-alkyl elimination (4) elimination, 1,2-rearrangement, and 2,1-insertion (Fig. 1, spectrum 5). In addition to the non-detected β-alkyl elimination, three other release mechanisms were detected for complexes 2, 3, and 4. β-hydride elimination was the main pathway for the chain release of complexes 1, 2, 3, and 4. The highest vinylidene content was found in 1 and the least in 4, which is consistent with the selectivity maintained by the dimer. We also found that using one-step activation and two-step activation did not change the chain-end release mechanism.

The reaction temperature is an effective way to control the degree of polymerization (DP_n). Increasing the temperature decreases the ratio of the chain growth rate constant to the termination rate constant. This is because it contributes to the elimination and termination of β hydride by chain transfer to Al [40], which results in a decrease in DP_n. This leads

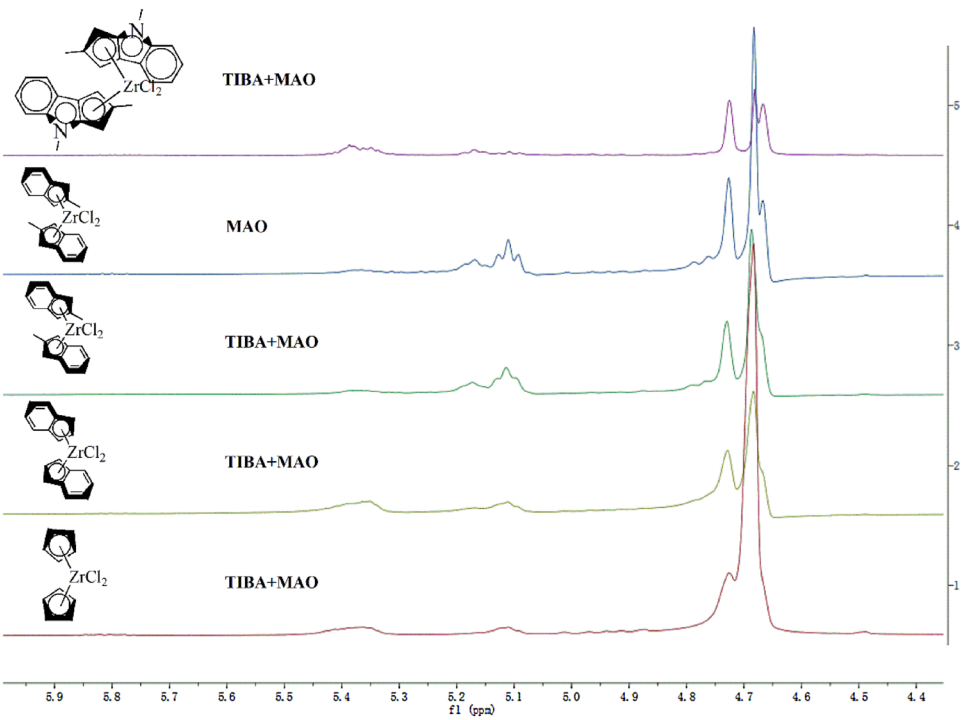

Fig. 1. ^1H NMR spectra (end group region) of poly-1-decene, obtained under argon atmosphere at 80 °C from 20 eq. of TIBA and 10 eq. of MAO activated under complexes 1, 2, 3 and N-doped complex 4

Table 2 Oligomerization of 1-decene at different temperatures (4 h, 20 eq. TIBA, 100 eq. MAO, 1-decene/Zr = 3×10^4)

Run	Cat	T,℃	Conv.,%[a]	% Selectivity of oligomers in the reaction mixture after 4 h, for P_n				M_n[c]	M_w[c]	KV^{40}, cSt	KV^{100}, cSt	VI
				2^b	3^b	4^b	5^b					
1	**3**	70	64.4	28.2	27.9	23.0	20.9	1288	4257	96.26	16.86	191
2		80	84.9	40.1	31.4	17.0	11.5	909	2383	33.31	7.13	185
3		90	85.6	46.5	28.5	15.3	9.7	753	2433	25.72	5.95	189
4		100	83.9	58.1	25.9	10.1	5.9	518	1048	10.54	3.08	165
5		110	82.9	82.2	13.4	3.4	0.9	406	603	6.38	2.15	157
6	**4**	60	85.9	12.2	21.6	24.9	41.3	3843	7048	625.29	74.83	201
7		70	87.6	20.9	24.1	25.0	30.1	2366	5108	311.22	41.8	190
8		80	90.0	22.6	27.0	25.0	25.5	1562	3440	129.97	21.18	189
9		90	86.6	27.6	27.2	24.5	20.6	1425	3390	96.39	16.7	189
10		100	85.0	36.7	27.0	18.9	17.5	993	1836	39.29	8.00	182
11		110	85.3	39.8	28.8	13.1	12.3	787	1655	27.76	6.14	179

[a]Polymerization conversion of olefins

[b]GC Data

[c]By GPC (THF)

to an increase in the dimer content. Therefore, the polymerization behavior of complex 3 and complex 4 was investigated at 60–110 °C, and the results are shown in Table 2.

For complex 3, the conversion was 64.44% at 70 °C and the highest conversion was obtained at 90 °C as 85.56%. Meanwhile, the selectivity of the dimer in the polymerization product increased from 28.21 to 82.22% with increasing temperature, a phenomenon that remained consistent with M_w. In addition, the value of KV^{100} of the polymer obtained at 110 °C for complex 3 was reduced to 2.15, at which point the product barely achieved lubrication. Fortunately, the N-doped complex 4, already reached 85.85% conversion at 60 °C, while complex 3 could be close to it at 90 °C. Importantly, the dimer selectivity of N-doped complex 4 grows slowly over the entire temperature range. In addition, complex 3 starts synthesizing lubricant base oils with low viscosity at 80 °C. Although, high viscosity lubricant base oils can be synthesized at low temperatures, the decrease in temperature leads to a sharp decrease in the conversion of the system. Surprisingly, complex 4 can obtain three different viscosities of lubricant base oils, high, medium and low, by facile temperature regulation in the range of 60–110 °C. Simultaneously, the VI values of the lubricant base oils obtained with N-doped complex 4 were all higher than 180.

3.3 Optimization of Catalytic Conditions

In order to investigate the optimal conditions for the performance of N-doped complex 4 in catalytic 1-decene polymerization, a series of modulation experiments were done. The experimental results are summarized in Table 3.

Analysis of the data in combination with Table 1 revealed that the highest unidirectional conversion has been achieved at 20 eq. of TIBA and 50 eq. of MAO for activation. To explore the effect of TIBA content on the catalytic activity. We found that insoluble N-doped complex 4 could not be fully activated when 5 eq. of TIBA was added to the system, leading to a decrease in activity. The polymerization conversion was 71.52% (Table 3, Run 8). The polymerization conversion was 91.3% with only 10 equivalents of TIBA (Table 3, run 9). As the concentration of TIBA increases, the conversion decreases slightly, the selectivity of the dimer decreases, and the selectivity of the pentamer increases. This led to an increase in M_w. This is in agreement with the work of Nifant'ev et al. [36]. However, changing either the concentration of MAO or TIBA has a much smaller effect on the viscosity of the product than the effect of temperature.

Figure 2 shows the variation of each unsaturated end group with temperature. In the temperature range studied, the chain end release mechanism forms only about 10–20% of the tri-substituted double bonds via 1,2 rearrangement. In contrast, the formation of internal –CH=CH– fragments via 2,1-insertion and the formation of vinylidene content via β-hydride elimination are very sensitive to temperature. The vinylidene end group dominates at higher temperatures and the internal –CH=CH– fragment dominates at lower temperatures (see Supporting Information for further support of unsaturated end-group assignment). This can be explained by the transfer rate [41]. Notably, with increasing temperature, a β-alkyl chain end release mechanism was detected. However, the mechanism for its appearance is unclear and needs further investigation.

Table 3 Optimization experiment of catalyst **4**

Run	T, ℃	Al_{MAO}/Zr	Al_{TIBA}/Zr	Conv., %[a]	% Selectivity of oligomers in the reaction mixture after 4 h, for P_n				M_n[c]	M_w[c]	KV^{40}, cSt	KV^{100}, cSt	VI
					2^b	3^b	4^b	5^b					
1	80	30	20	82.3	25.1	31.1	25.6	18.3	1207	2394	61.86	11.35	180
2	80	70	20	89.8	23.0	28.9	26.3	21.8	1828	3010	93.83	15.84	181
3	50	50	20	73.1	9.5	19.3	22.5	48.6	6557	11,227	1274.94	119.56	194
4	60	50	20	83.2	14.3	26.2	29.9	29.7	2391	5136	342.26	44.47	188
5	70	50	20	85.7	18.8	31.6	23.9	25.8	1884	4238	219.12	31.84	190
6	90	50	20	85.3	35.9	27.0	19.2	17.9	1141	2552	54.83	10.25	180
7	100	50	20	86.0	39.8	28.8	13.1	12.3	857	1639	30.39	6.56	179
8	75	50	5	71.5	25.0	28.0	25.4	21.6	1452	3169	103.53	17.45	186
9	75	50	10	91.3	25.5	26.8	24.5	23.2	1605	3378	120.56	20.58	196
10	75	50	15	89.9	25.6	29.9	21.2	23.4	1597	3518	125.59	21.54	199
11	75	50	20	88.4	24.5	28.7	22.2	24.6	1827	4173	152.13	24.63	195
12	75	50	30	86.6	20.0	25.9	27.5	26.6	2063	4512	217.82	32.47	195
13	75	50	40	83.7	20.1	24.9	27.8	27.2	2270	4287	209.89	29.75	183
14	75	50	100	83.0	18.8	24.4	29.0	27.8	2327	5138	334.85	44.75	193

[a]Polymerization conversion of olefins

[b]GC data

[c]By GPC (THF)

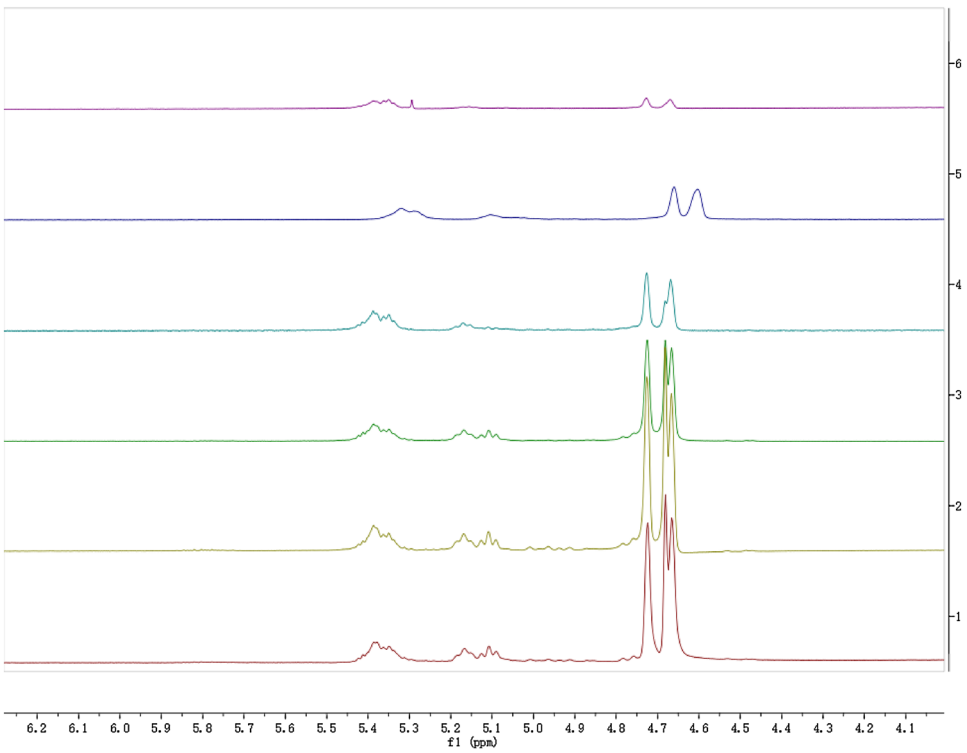

Fig. 2. ^1H NMR spectrum of poly-1-decene (end group region) in the presence of N-doped complex 4 under argon atmosphere. Obtained by polymerization experiments at 50–100 °C (top–bottom)

In addition to this we analyzed the stereochemical structure of the resulting poly(1-decene). As expected, complex 4 (C_2) symmetrically catalyzed the atactic polymerization of 1-decene (Supporting Information, Fig. S7 provides the ^{13}C NMR spectrum).

4 Conclusions

In summary, we investigated the catalytic activity of insoluble 2,4-dimethyldihydrocyclopentadienyl[b]indole-derived N-doped compound $LZrCl_2$ as well as soluble complexes 1,2,3 in the polymerization of 1-decene. One-step activation method and two-step activation method were compared. It was found that the product dimer selectivity of the one-step activation method increased with increasing Al/Zr, while the two-step activation method exhibited the opposite trend. And the two-step activation method greatly improved the polymerization activity and led to a significant increase in the VI of the PAO base oils. The possible reaction pathways for α-olefin oligomerization are summarized. The oligomers formed are mainly dominated by vinylidene chain ends. The resulting unsaturated chain ends are produced by 1,2-rearrangement and β-hydride elimination or 2,1-insertion as well as β-hydride elimination.

The conditions for the polymerization of N-doped complex 4 were optimized. High catalytic activity was also achieved at Al_{MAO}/Zr~10. By varying the concentrations of TIBA and MAO, the highest polymerization conversion was obtained at a reaction temperature of 75 °C with 10 eq. of TIBA and 50 eq. of MAO activation. High activity at low temperatures and good tolerance to high temperatures were found by varying the reaction temperature. It has excellent viscosity modulation in the region of high activity and stable reaction temperature. The product of 1-decene polymerization catalyzed by N-doped complex 4 has very low dimer selectivity and high VI. It is a promising single-site catalyst for α-olefin oligomerization.

Supplementary Information The online version contains supplementary material available at https://doi.org/10.1007/s10562-023-04333-y.

Acknowledgements We especially acknowledge the support of National Natural Science Foundation of China (22072175) and the Strategic Pioneer Special Fund of the Chinese Academy of Sciences (XDA29030402).

Declarations

Conflict of interest The authors declare no conflict of interest.

References

1. Yadav GD, Doshi NS (2002) Green Chem 4:528–540
2. Ray S, Rao PVC, Choudary NV (2012) Lubr Sci 24:23–44
3. V.I. Andrianov (1987) Kristallografiya 32
4. MaijaLahtela TAP, Nissfolk F (1995) J Phys Chem 99:10267–10271
5. Nifant'ev IE, Vinogradov AA, Vinogradov AA, Sedov IV, Dorokhov VG, Lyadov AS, Ivchenko PV (2018) Appl Catal A Gen 549:40–50
6. Nagendramma P, Kaul S (2012) An overview. Renew Sustain Energy Rev 16:764–774
7. Carpenter JF (1995) J Synth Lubr 12:13–20
8. Bae JS, Hong SY, Park JC, Rhim GB, Youn MH, Jeong H, Kang SW, Yang JI, Jung H, Chun DH (2019) Appl Catal B Environ 244:576–582
9. Wan HL, Gong NF, Liu LC (2022) Sci China Chem 65:2163–2176
10. Kissin YV, Schwab FC (2009) J Appl Polym Sci 111:273–280
11. Shao HLH, Lin J, Jiang T, Guo X, Li J (2014) Eur Polym J 59:208–217
12. Huang LCQ, Ma L, Fu Z, Yang W (2005) Eur Polym J 51:2909–2915
13. Grumel V, Brull R, Pasch H, Raubenheimer HG, Sanderson R, Wahner UM (2001) Macromol Mater Eng 286:480–487
14. Babushkin DE, Semikolenova NV, Zakharov VA, Talsi EP (2000) Macromol Chem Phys 201:558–567
15. Kaminsky W (2012) Macromolecules 45:3289–3297
16. Margaret May-Som Wu CLC, Walzer Jr JF, Jiang P (2007) U. S. Patent, US8207390
17. Nifant'ev IE, Ivchenko P, Vinogradov AA (2021) Coordin Chem Rev 426:213515
18. Nifant'ev IE, Ivchenko P (2020) Adv Synth Catal 362:3727
19. Nifant'ev IE, Vinogradov AA, Vinogradov AA, Bagrov VV, Churakov AV, Minyaev ME, Kiselev AV, Salakhov II, Ivchenko PV (2022) Mol Catal 529:112542
20. Wang Jiannan LM, Yilong C, Abbas M, Jiangang C (2022) China Pet Process PE 24:52–60
21. Balboni D, Camurati I, Prini G, Resconi L, Galli S, Mercandelli P, Sironi A (2001) Inorg Chem 40:6588–6597
22. Grimmer NE, Coville NJ, de Koning CB, Smith JM, Cook LM (2000) J Organomet Chem 616:112–127
23. van Baar ADHJF, de Kloe KP, Kragtwijk E, Mkoyan SG, Nifant'ev IE, Schut PA, Taidakov IV (2003) Organomet 22:2711–2722
24. Bergman JEBJ (1975) Tetrahedron 31:2063–2073
25. Fan GQ, Dong JY (2005) J Mol Catal A Chem 236:246–252
26. Nifant'ev IE, Vinogradov AA, Vinogradov AA, Churakov AV, Bagrov VV, Kashulin IA, Roznyatovsky VA, Grishin YK, Ivchenko PV (2019) Appl Catal A Gen 571:12–24
27. Christoffers J, Bergman RG (1996) J Am Chem Soc 118:4715–4716
28. Christoffers J, Bergman RG (1998) Inorg Chim Acta 270:20–27
29. Brant P, Jiang P, Lovell J, Crowther D (2016) Organomet 35:2836–2839
30. Janiak C, Lange KCH, Marquardt AP, Kruger RP, Hanselmann R (2002) Macromol Chem Phys 203:129–138
31. Kawahara N, Saito J, Matsuo S, Kaneko H, Matsugi T, Toda Y, Kashiwa N (2007) Polymer 48:425–428
32. Jalali A, Nekoomanehs-Haghighi M, Dehghani S, Bahri-Laleh N (2020) Appl Organomet Chem 34
33. Dehghani S, Hanifpour A, Nekoomanesh-Haghighi M, Sadjadi S, Mirmohammadi SA, Farhadi A, Bahri-Laleh N (2020) J Appl Polym Sci 137

34. Nifant'ev IE, Vinogradov AA, Vinogradov AA, Bezzubov SI, Ivchenko PV (2017) Mendeleev Commun 27:35–37
35. Shao HQ, Li H, Lin JC, Jiang T, Guo XY, Li J (2014) Eur Polym J 59:208–217
36. Nifant'ev IE, Vinogradov AA, Vinogradov AA, Ivchenko PV (2016) Catal Commun 79:6–10
37. Nifant'ev IE, Ivchenko P, Tavtorkin A, Vinogradov A, Vinogradov A (2017) Pure Appl Chem 89:1017–1032
38. Nifant'ev IE, Vinogradov A, Vinogradov A, Karchevsky S, Ivchenko P (2020) Polymers-Basel 12
39. Nifant'ev IE, Vinogradov A, Vinogradov A, Karchevsky S, Ivchenko P (2019) Molecules 24:3565
40. Fan Z-Q, Yasin T, Feng L-X (2000) J Polym Sci Part A-Polym Chem 38:4299–4307
41. Zhao X, Odian G, Rossi A (2000) J Polym Sci Part A-Polym Chem 38:3802–3811

Authors and Affiliations

Bingyu Shi[1,2] · Man Liu[1] · Jiangang Chen[1]

✉ Man Liu
liuman@sxicc.ac.cn

✉ Jiangang Chen
chenjg@sxicc.ac.cn

[1] State Key Laboratory of Coal Conversion, Institute of Coal Chemistry, Chinese Academy of Sciences, Taiyuan 030001, Shanxi, People's Republic of China

[2] University of Chinese Academy of Sciences, Beijing 100049, People's Republic of China